Journal of Materials and Engineering Structures

Research Paper

The effect of the solar wall heating on the flow structure within the cross-ventilation of isolated building

Bendida Medjahed [a,*], ***Abdelkrim Benlefki*** [b,c], ***Mohamed Hamel*** [c]

[a] *Laboratory of Numerical and Experimental Modeling of Mechanical phenomena, University of Abdelhamid Ibn Badis, Faculty of Science and Technology , Mostaganem, Algeria.*

[b] *Department of Science and Technology, Tissemsilt University , Algeria.*

[c] *Laboratory of Applied Mechanics; University Of Science and Technology of Oran, Faculty of Mechanical Engineering, BP. 1505 El-Mnaouar, Oran, Algeria.*

ARTICLE INFO

Article history:

Received : 5 August 22

Revised : 24 December 22

Accepted : 8 January 23

Keywords:

Thermal

Cooling or heating a building

Isolated building

Numerical simulation

Air quality

ABSTRACT

In this paper a comprehensive study is conducted on the heat transfer between building and the atmosphere within a cross ventilation situation, this situation is characterized by a transverse flow between the two parallel windows of an isolated building. The study is divided into two parts, in the first part, the effect of the walls, solar heating during the day (windward between sunrise and noon, the roof at the moon and leeward between noon and sunset) on the air temperature distribution and air velocity inside and outside an isolated building is studied when a numerical simulation is conducted in an atmospheric micro scale. For the second part, the study is focused on the effect of temperature change of the building floor, by an external heating source such as a recessed serpentine, on cooling or heating the air but in this case only inside the building by numerical simulation. The numerical results are validated using experimental measurements (velocity profiles and turbulent kinetic energy) of Y. Tominaga realized at Niigata Institute of Technology in Japan, these measurements provide a very useful database for validation of numerical models of computational fluid dynamics (CFD). Compared to those wind tunnel experimental measurements, the numerical results of the cross-ventilation show a good agreement. The detailed results analysis shows that the differential heating of all building surfaces can greatly influence the capacity of the flow to transport and exchange heat.

1 Introduction

The needs of heating and cooling buildings are strongly associated with the micro-climatic conditions that develop nearby it is therefore important to consider thermal convection and in particular the influences due to direct solar radiation in inside a building, this is why this study is presented. As only a limited number of researchers in this field have studied

* *Corresponding author. Tel.: +213655203399.*
E-mail address: medjahedb@gmail.com

e-ISSN: 2170-127X,

RESEARCH REVIEW of Sciences and Technologies

numerically the influence of dynamic parameters on the temperature distribution, thermal comfort, none of them dealt with the case of natural cross ventilation in an isolated building with two openings in the center of windward and leeward. For example, Stavrakakis et al. 2008 [1] evaluated the thermal comfort in an applied isolated building with two non-symmetrical openings exposed to solar radiation, numerical simulation used the standard k-ε and realizable k-ε turbulence models to assess the velocity and temperature fields inside and outside the building and an experimental study was carried out to measure the convection exchange coefficient around a human (manikin) [2]. To improve natural ventilation, researchers such as Del Rio and others took a model applied in the city of Kumagaya, Japan, on which they conducted a study and evaluation of the method of cooling the internal air of an isolated house, and they concluded that thermal comfort is affected by the change of external climatic factors and this is greatly [3]. Operating a heat source in addition to the heat emitted from electrical appliances inside the home daily has a great impact on the thermal comfort of standing and sitting because it uses a very large amount of energy and this was deduced from the results of the numerical study presented by Sherzad Hawendi and others [4]. Yongling et al. he gave a presentation on the effect of thermal comfort on the population, as well as the energy consumed for indoor air conditioning [5]. In this study, Yi Wang presents a numerical simulation in which he focuses on the thermal aspect and the extent of its effect on the dispersion of pollutants between two adjacent industrial workshops [6]. The researchers, Yatharth Vaishnan et al., [7] Concluded that the availability of suitable roof angles gives better ventilation rate and good air circulation pattern, and greatly affects the comfort and heat inside the buildings. Where they focused in their study on the angle of inclination of the roof and thermal comfort and chose the three different weather conditions in the city of Delhi (winter season, summer season, and monsoon season). The research showed by numerical simulation the flow regimes and the precise thermal environment were examined in the Canyon models. The solar ray tracing model was performed to study the turbulence properties using wind-induced force and solar heating conditions. This work indicates that it provides a reference for future urban planning and is of great importance [8]. The older experimental studies one can find the study of Straw et al. [9] and Karava et al. [10]. The first [9] present an experimental, theoretical and numerical investigation of the surface pressure coefficient, the average and the total ventilation rates in a cube with a dimension of 6m. The second [10] added in an experimental study the discussion of the discharge coefficient evaluated as a function of external and internal pressure coefficient, the reference velocity, the local velocity (at the entrance to the opening) and the mass flow through the cube. A significant number of researchers have studied experimentally and analyzed the cross-ventilation of an isolated and protected building with and without the pollutant's dispersion for several geometric and dynamic configurations [11, 12]. The study o Tominaga et al. [11]present an experimental analysis of the CH4 dispersion within a cross-ventilation in 5 cases of positions openings, the visualization is carried out for 16 seconds with measurements each 1 second. The present study is only interested to the first case of Tominaga et al. [12]. The most recent experimental studies [11, 13, 14] interested in cross-ventilation not for an isolated building but for a protected one (surround by a set of identical building). For example, in the experimental studies of Mohammadreza Shirzadia et al. [14] of building surrounding by eight buildings were presented against different wind angles. In this study we chose the large eddy simulation (LES), because this kind of prediction requires a high grid resolution, but the main jet direction, defined by an angle α is visible by the LES and SST model. Numerical studies of cross-ventilation have been more advanced using more detailed geometric and dynamic configurations compared to experimental studies which have been the validation reference. In addition to the detailed numerical data given by Von Hoff et al. [15] and Tominaga et al. [11]. Perén and others presented several studies of an insulated dent roof building and the extent of the effect of roof geometry on the building's internal ventilation. The first pedal consists of a general toothed roof isolated in the direction of the wind (Windward eaves, leeward eaves and eaves inclination), and the second one consists of a toothed roof isolated in the direction of the wind by cross ventilation (straight roof, concave roof, hybrid or convex roof) [16, 17]. Other studies can also be found in the literature, such as the experimental and numerical study of the cross ventilation of a building equipped with louvers in four cases of open position in four cases of opening position [18]. White the same methods, pressure, velocity and deviation of flow was investigated numerically by Chinchun, et al. 2019[19]. Otherwise, the impact of the guide vanes is studied by Arinami et al.[20, 21]. As for nanotechnology in the fields of direct absorption solar energy, a number of researchers in this field have conducted scientific studies such as Hussein A. and others, who provided a comprehensive and detailed overview and analysis of recent results related to this field, and they found that the use or application of this field can play a decisive role in increasing the efficiency of these devices [22, 23]. Eltahir K et al. they provided a detailed presentation on the energy performance and optimum thickness of the thermal insulation of buildings under Sudan's climate zones. Therefore, in this study, they chose to calculate the optimum thickness of thermal insulation for four selected cities in Sudan, where each city has different climatic conditions. Three different insulating materials are used, and this is to calculate the ideal thickness of the insulation in the outer wall, namely:

(extruded polystyrene, expanded polystyrene, and glass wool). These insulating materials have been applied to three different types of walls: (baked clay brick wall, red perforated brick wall, and hollow concrete block wall) [24].

2 Methodology

2.1 Experimental datasets

Documented experimental datasets produced in the wind tunnels of the Niigata Institute of Technology in Japan University were used in this study Wind tunnel experiments on cross-ventilation flow of building isolated. These datasets included wind and turbulence fields around isolated building. The different dimensions of building (0.2m x 0.2m x 0.16m) which was studied in the Niigata Institute wind tunnel [11]. In figure 01 shows the building shape and the location of the windward and leeward facade central openings with the wind direction of the same height level h = 80 mm.

2.2 Numerical models

ANSYS CFX is a general-purpose CFD model that has been used in a wide range of on cross-ventilation flow of building isolated and other engineering applications. The Reynolds Averaged Navier-Stokes CFD (i.e. Computational Fluid Dynamics) using the RANS approach with two-equation eddy viscosity turbulent model (k-ω SST). In this work, the CFD model (ANSYS CFX) that which have been used to simulate dynamic (wind flow) and the thermal effects . After the validation of the dynamics results of the ventilation with the experimental measurements, the same simulation parameters are preserved and the windward wall is heated.

2.3 Computational domain.

The domain of the simulation is a numerical wind tunnel of 1.8mx3.8mx0.96m with a cube of 3.08 m of length, a 1.8m of with and 0.96 m in the height; the same dimensions are used in the experimental study of Tominaga et al. [11]. The figure 1 presents all the important dimensions.

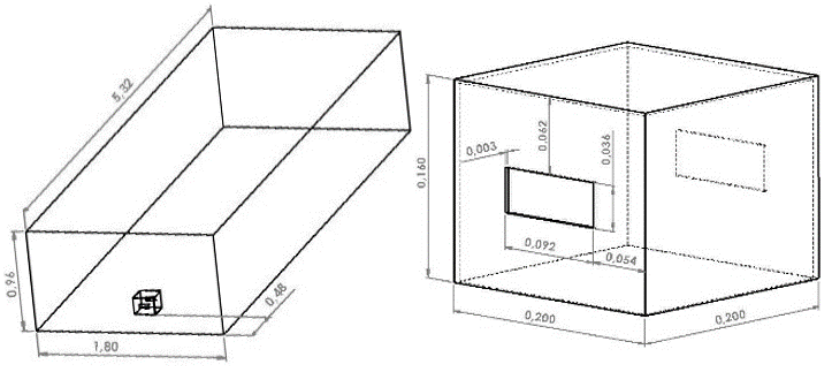

Fig. 1 – Computational domain and building geometry (Dimension in m)

2.4 Problematical

Solar radiation has a direct and remarkable impact on thermal comfort and consequently on the dynamic situation as well as on air conditioning and heating installations. This impact is becoming more and more important in areas where sunshine lasts for several hours a day, particularly in the Saharan regions. The quantitative knowledge of the heat flows exchanged between the external environment and inside and their effects on the dynamic behavior of the air participates in an effective way to reduce the installation bill and the exploitation of the energy systems which provide comfort.

In the first part, four ideal cases of a sunlit wall are studied (Figure 2). The first case the isothermal (all walls same the ambient air temperature); the second case the temperature of either the ceiling and the interior wall for ceiling is set to 30°C; the third case the windward wall and the interior wall for him is set to 30°C and the last case the leeward wall and the interior wall for him is set to 30°C, while the thermal stratification of the inflow is neutral and the ambient air temperature

at ground level is 20°C and in all casses (Tw - Tair) = 10 °C). The other inflow conditions and the calculation grid are exactly the same as for the previous simulations. In This figure 2-1 shows the four configurations that have been studied. In the first case we see a cloudy sky. As in the other cases, we find a sunny sky, we therefore choose the positions of the sun three times during the day, the second case in the morning around 8:30 a.m., the third case at noon around 1 p.m. and in the fourth case in the evening around 17h 30 min. As for the second part, we have studied the effect of temperature (air and floor) on cooling or heating a building inside for this reason we conducted a numerical study about study the effect of temperature (air and floor) on cooling or heating a building inside. The aim of this part of the thermal study is to determine the final results of cooling or heating a building from the inside in order to present serious solutions to this problem. For that, we made several numerical simulations concerning thermal part by software ANSYS CFX. the first case we have each time changed the air temperature and fixed the indoor floor temperature for an insulated building [(Ta = 55 ° C and Tf = 20 ° C), (Ta = 40 ° C and Tf = 20 ° C)], the second case we have fixed the two temperatures of the air and the indoor floor temperature (Ta = 20 ° C and Tf = 20 ° C) and the third case we have fixed the temperature of the air and changed each times the indoor floor temperature [(Ta = 20 ° C and Tf = 30 ° C), (Ta = 20 ° C and Tf = 45 ° C)] (see figure 2-2).

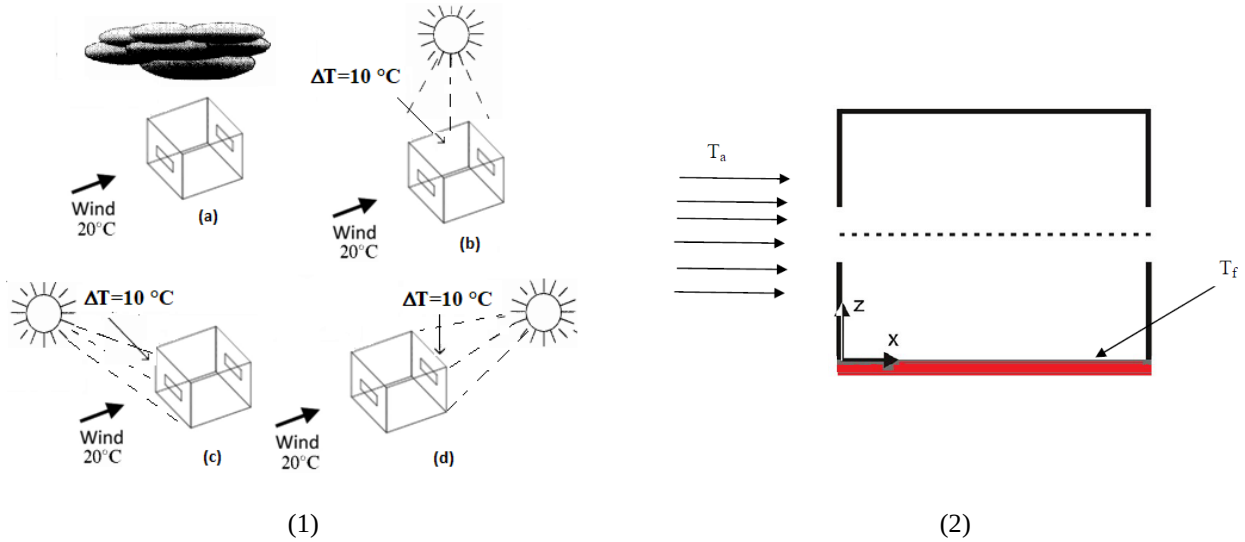

Fig. 2 – Work area divided by two parts: (1) In the first part the sunlit wall configurations and air flow with: (a) isothermal reference case, (b) ceiling heating reference case, (c) windward heating reference case and (d) leeward heating reference case, (2) for the second part the temperature (air and floor) on cooling or heating a building inside

2.5 Simulation grids

The ANSYS ICEM is used to create the grids of simulation. As it is shown in Fig.3 the simulation grid mesh is composed by titrahydric cells and in order to have $y_{plus}< 2$, in accordance with the turbulent model used (k-ω SST) some prism layers near the walls and high mesh density inside the building are generated.

2.6 Boundary conditions

In order to compare the numerical results of the dynamic part of this study with the experimental results of Tominaga et al. [11] carried out in atmospheric wind tunnel at Niigata institute of technologies, Japan, the numerical and experimental boundary layers are the same with using the flowing expression:

$$U(z) = \frac{u^*_{ABL}}{\kappa} \ln\left(\frac{z+z_0}{z_0}\right) \quad (1)$$

The turbulent kinetic energy (k) was calculated from the expression:

$$\frac{k(z)}{U_H^2} = 0.033\exp^{-0.32\left(\frac{z}{h}\right)} \quad (2)$$

The energy dissipation at the inflow boundary (ε) was calculated from the expression:

$$\varepsilon(z) = \frac{(u^*)^3}{\kappa(z+z_0)} \tag{3}$$

The z the vertical axe coordinate, the z0 represent the aerodynamic roughness, u* is the friction velocity of the AB Land κ the Von Karman constant (κ=0.42),

$$\omega(z) = \frac{\varepsilon(z)}{C_\mu k(z)} \tag{4}$$

H is the building height and it is egal 0.16m, UH is the flow velocity at H, Cμ is a constat (Cμ=0.09) and k is the turbulent kinetic energy.

A summary of model boundary and inflow conditions is presented in Table 1.

Table 1 – Aerodynamic wall roughness (Zo), friction velocity (u*), reference velocity (UH) at height Zref for the for the building.

	Z_0 (m)	u* (m/s)	U_H (m/s)	Z_{ref} (m)
Wind tunnel	0.0009	0.348	4.3	0.16
CFX-Pre	0.0009	0.348	4.3	0.16

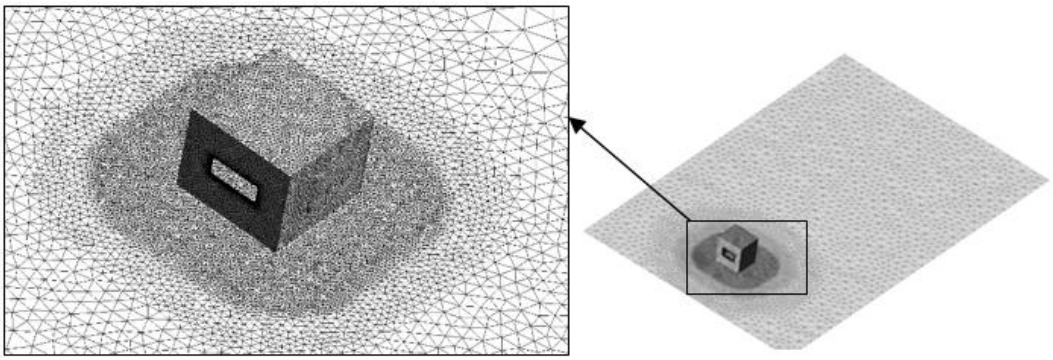

Fig. 3 – Computational grid on the building and the bottom of the domain with a zoom on building surfaces showing the density grid zone

3 Test and analysis of grids

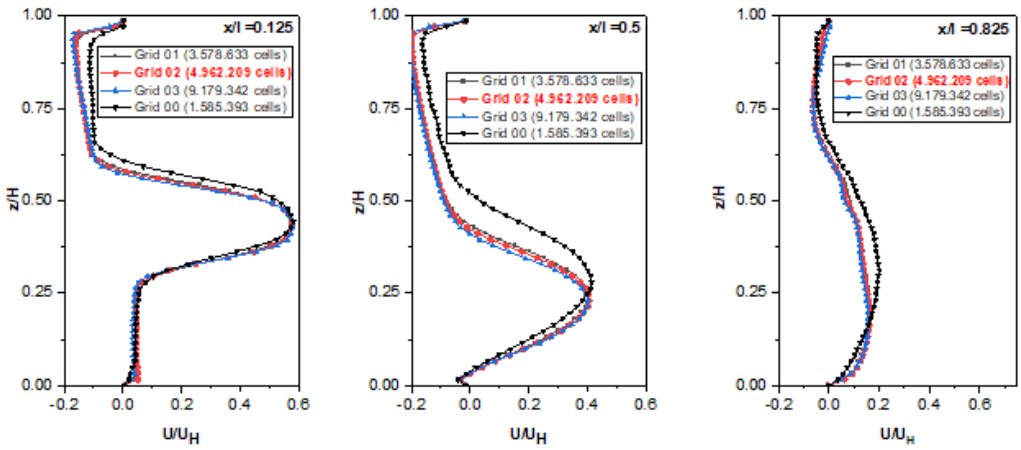

Fig. 4 – Tested of the vertical profiles of velocity (U/Uh). Four grids are used, the coarse grid (Grid0 equal to 1.585.393 cells), basic-1 (Grid1 equal to 3.578.633 cells), basic-2 (Grid 2 equal to 4.962.209 cells) and the fine grid (Grid 3 equal to 9.179.342 cells) at three line positions. a) x/l =0.125, b) x/l =0.5, c) x/l =0.875.

When simulating finite volumes, a finer mesh generally produces a more precise solution. In return, this finer mesh increases the calculation time. In this study we made four meshes, the coarse grid (Grid0 equal to 1.585.393 cells), basic-1 (Grid1 equal to 3.578.633 cells), basic-2 (Grid 2 equal to 4.962.209 cells) and the fine grid (Grid 3 equal to 9.179.342 cells). The figure 04 represents a tested of the vertical profiles of velocity and a comparison of four grids at three line positions. a) x/l =0.125, b) x/l =0.5, c) x/l =0.875. On the basis of this comparison and analysis it was judged that the basic-2 grid (Grid 02) is judged the optimal grid for the validation for the continuation of the dynamic computation in this article.

4 Numerical results validation

A comparison of the current numerical results of the dynamic parameters of the cross-ventilation in the building with those carried out experimentally by Tominaga et al [11] is analyzed and presented in the fig.5. the vertical profiles of the horizontal dimensionless velocity component (u/uh) is plotted along seven positions inside the building, x/l=0.125, x/l=0.25, x/l=0.375, x/l=0.5, x/l=0.625, x/l=0.75, x/l=0.875 at the central plan (y/x=0), in accordance with the experimental measurements. At the entrance of the building (x/l=0.125, x/l=0.25, x/l=0.375, x/l=0.5), the numerical results are very comparable to the experimental ones but after the middle line point there is little difference between the numerical results and experiment.

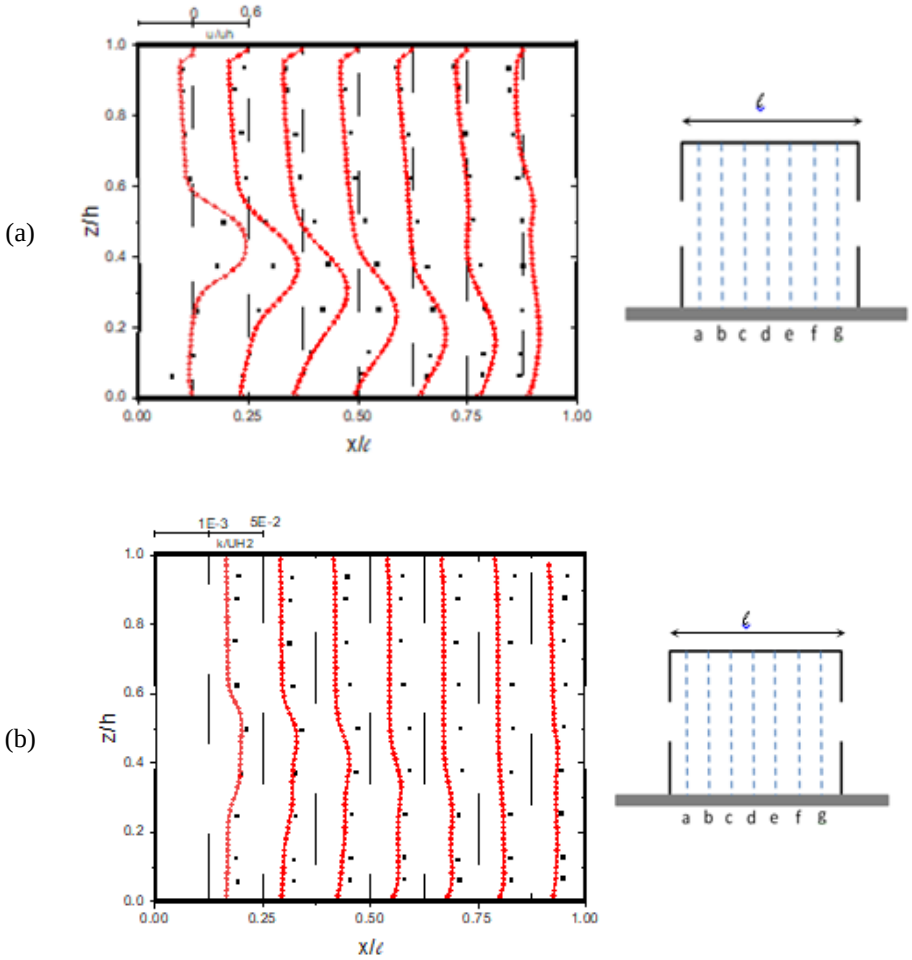

Fig. 5 – Comparison of experimental and numerical simulation; (a) velocity (U/Uh) vertical profiles normalized and (b) the dimensionless turbulent kinetic energy (k/Uh2), for seven line positions along the building on the central plane. a) x/l=0.125, b) x/l=0.25, c) x/l=0.375, d) x/l=0.5, e) x/l=0.625, f) x/l=0.75, g) x/l=0.875.

The comparison of the numerical and the measurements of the turbulent kinetic energy on the dimensionless form (k/U_h^2) are provided in Fig.6, at the same plan and the same point as Fig.5. In all points lines of the vertical profiles the numerical values of the turbulent kinetic energy are underestimated regarding to the measurements except in the zone of the

jet flow when the intensity of turbulence is very important. This is due to ability of the model used to capture the intense perturbations, but out of the jet zone the comparison shows a difference between numerical and experimental results.

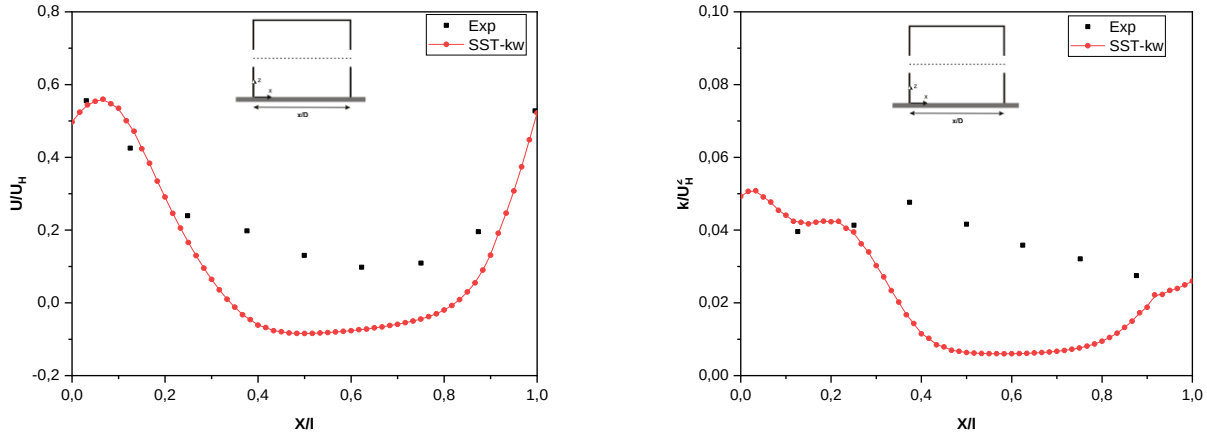

(a) (b)

Fig. 6 – Comparison of experimental and numerical simulation; (a) velocity (U/Uh) horizontal profiles normalized and (b) the dimensionless turbulent kinetic energy (k/U²h), for line position of the building z/h=0.08 on the central plane.

4.1 The effect of wall and ceiling temperatures on vertical exchanges between layers of air within a building

This section aims to answer the following question: What are the effects of the heat flow of a wall or ceiling due to solar heating of a building on heating the walls of an insulated building from the inside?

There are a few experimental results of the research that allow an answer to this question and most of the wind tunnel simulations of urban isothermal flows. With regard to the atmosphere over the roofs, measuring the internal values of wind speed, direction, and air temperature, as well as the temporal evolution of temperature inside the building, air flow and more, some researchers considered that according to the hour of the day, the direction of the vortex varies according to the conditions of the sun's brightness. The objective of this section is to assess the effect of wall and ceiling temperatures on vertical exchanges between layers of air within a building. Therefore, three ideal sunlit wall configurations are simulated (Figure. 2). The ceiling, windward, leeward wall is set at 30 ° C (see figure 2.b, 2.c and 2.d), while the internal flow thermal stratification is neutral and the ambient air temperature at ground level is 20 ° C. In this simulation the other flow conditions and the calculation network are exactly the same as the previous simulations.

4.2 Results and discussion

A numerical model was built to numeric simulate micro-scale atmospheric flows in an isolated building based on the classical lower micro-scale atmospheric and the turbulence model (k-w SST). This CFD model is used here to study the vertical thermal flows and exchanges within an isolated building in three cases (the ceiling reference case, the wind reference case and the downwind reference case).

Figure 7 provides the average velocity field in a vertical mid-plane and velocity vector and the main observation it is in three cases (the ceiling reference case, the downwind reference case and the leeward reference case) there is no visible difference between any of these cases from the simulation results and they all look identical, where we note that at the speed contours in the central plane approximately they have the same orientation at the entrance or inside the building, as well as at the exit hole. Simply because in this numerical simulation we apply the same conditions of entry and the boundary conditions in the three cases.

Figure 8.a shows a comparison of velocity (U/Uh) by turbulence model (k-ω SST) with three different cases, the first case ceiling heating reference, the second case windward heating reference, and the third case leeward heating reference along twelve vertical lines on a vertical mid-plane (y/l = 0) among them are seven inside the building. The main observations are:

- The turbulence model (k-ω SST) provides accepted results to the corresponding measurements. Then the flow dynamic of the cross ventilation of the studied case is validated with success, but the turbulent kinetic energy for the same case using the same model is presents some differences numerical and experimental results inside the building, these differences are also in almost all numerical studies of similar case

- In all three cases (ceiling heating reference case, windward heating reference case and leeward heating reference case), all the vertical velocity profiles outside or inside the building are founded roughly the same shape of the graphs because of the same boundary conditions.

- The k-ω SST model provide about the same vertical location of maximum U/Uh in the jet region along each vertical line. It is remarkable that the k-ω SST model provide almost identical velocity profiles.

- The k-ω SST model provides values for the maximum velocity in the jet region; e.g. at x/l = 0.375 U/Uh =0.58.

-The general flow pattern in the lower part of the enclosure is better reproduced by k-ω SST (better prediction of vertical location of maximum velocity), while air flow at the top of the building (z/h > 0.5) is more accurately reproduced.

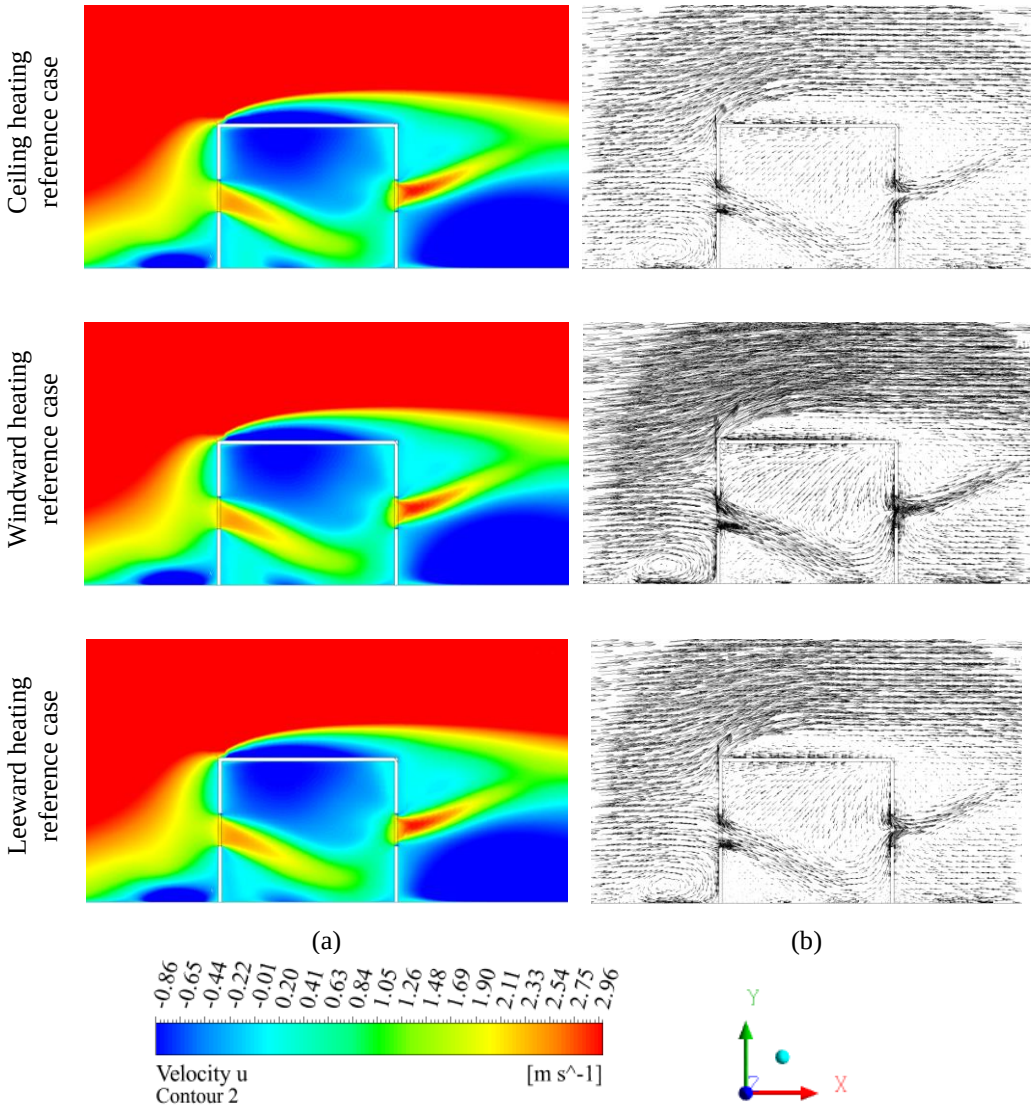

Fig. 7 – Cross sectional view of: (a) mean velocity field, (b) mean velocity vector field on a vertical mid-plane.

(1) Ceiling heating reference case

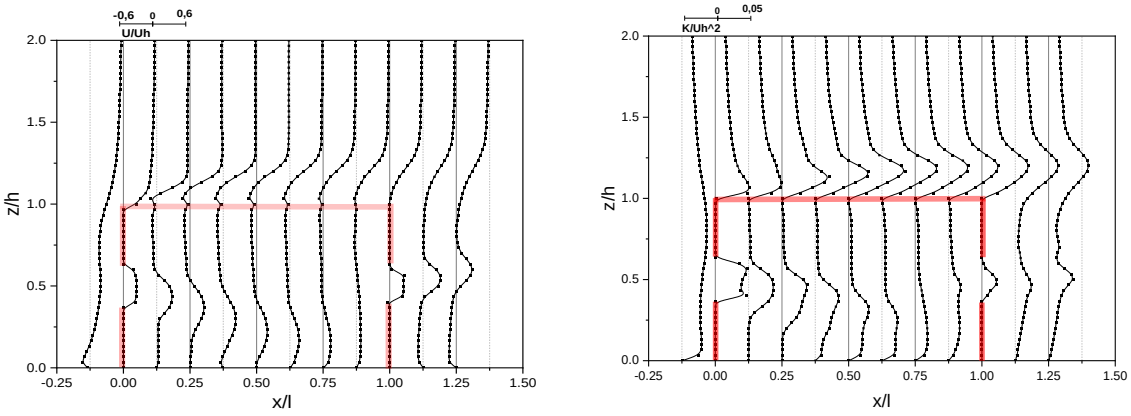

(a) (b)

(2) Windward heating reference case

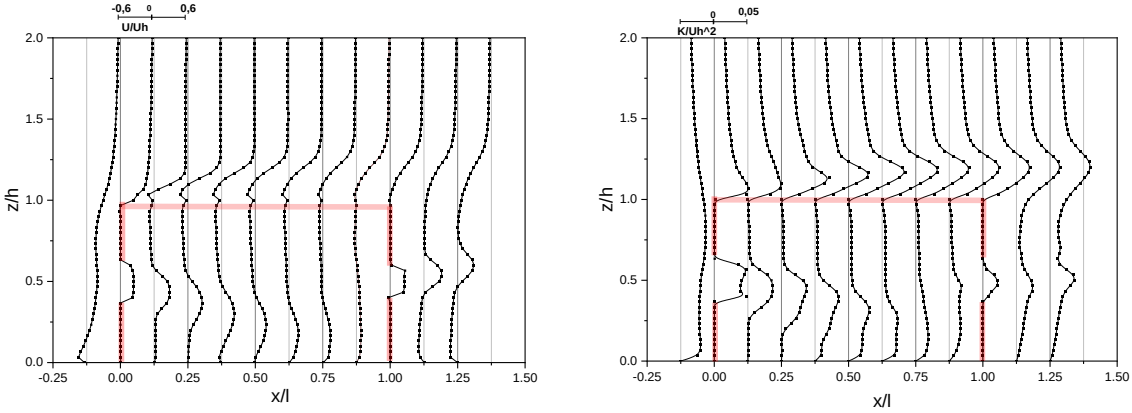

(a) (b)

(3) Windward heating reference case

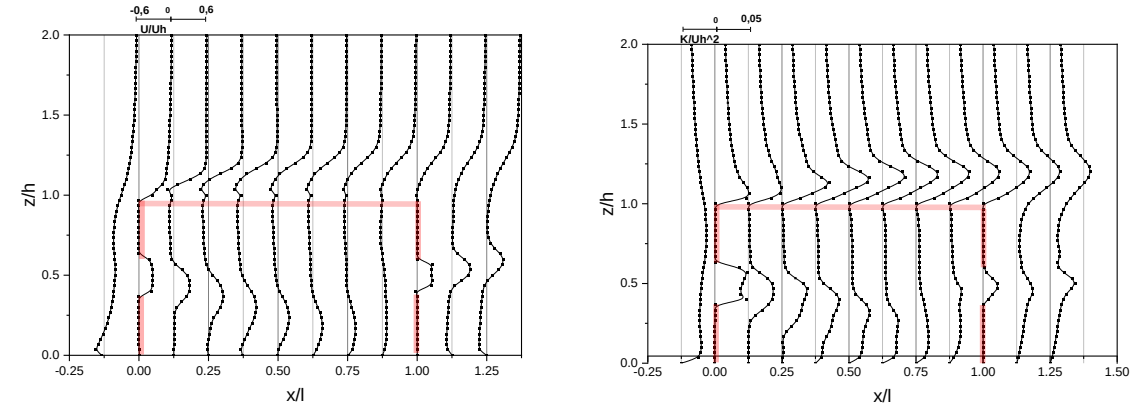

(a) (b)

Fig. 8 – Comparison Different profiles of a) averaged velocity (U/Uh) and b) turbulent kinetic energy (k/ Uh2) in vertical center section of unsheltered building for seven line positions along the building on the central plane. a) x/l=0.125, b) x/l=0.25, c) x/l=0.375, d) x/l=0.5, e) x/l=0.625, f) x/l=0.75, g) x/l=0.875.

Figure 8.b provides a comparison of the dimensionless turbulent kinetic energy (k/Uh2) along twelve vertical lines on a vertical mid-plane (y/l = 0) among them are seven inside the building. The most important conclusions we find are:

- The turbulence model (k-ω SST) does not correctly model the effect of transient flow features on the resolved turbulent flow inside the building.

- The turbulence model (k-ω SST) predicts the lowest values of turbulent kinetic energy in the jet region at x/l = 0.125 and x/l= 0.25 and provides an accepted coordination with the simulation results observed in Figure 8.b.

(1) Ceiling heating reference case

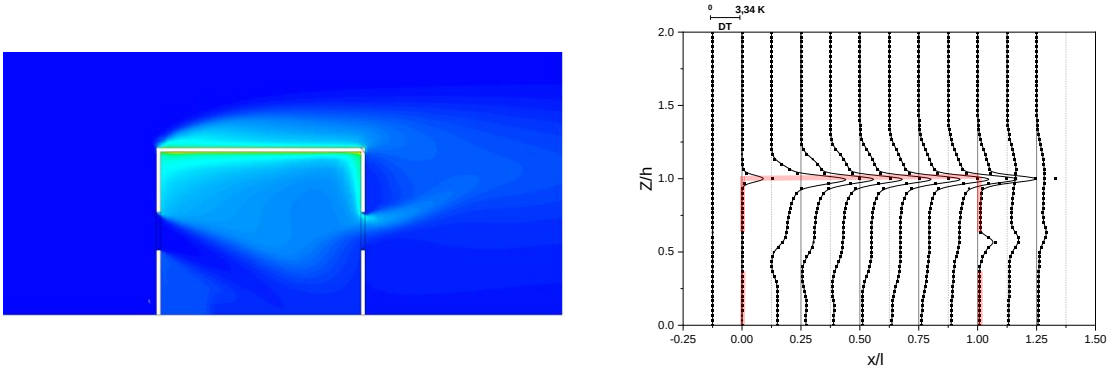

(2) Windward heating reference case

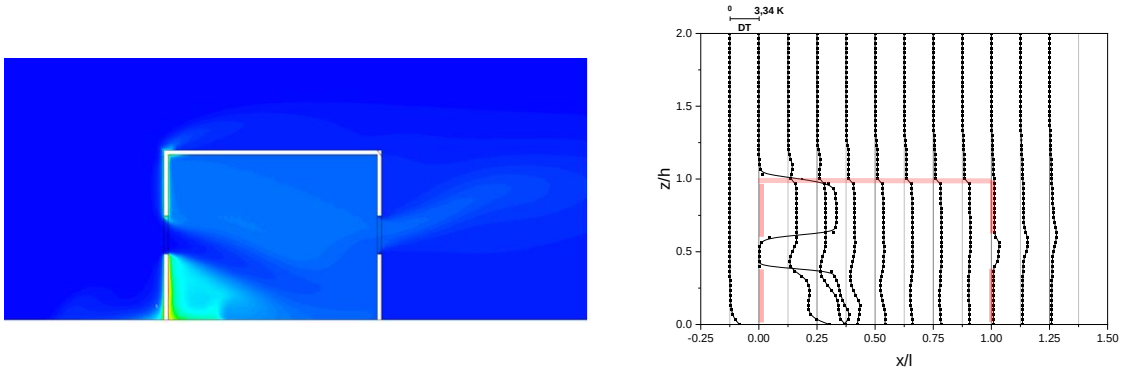

(3) Leeward heating reference case

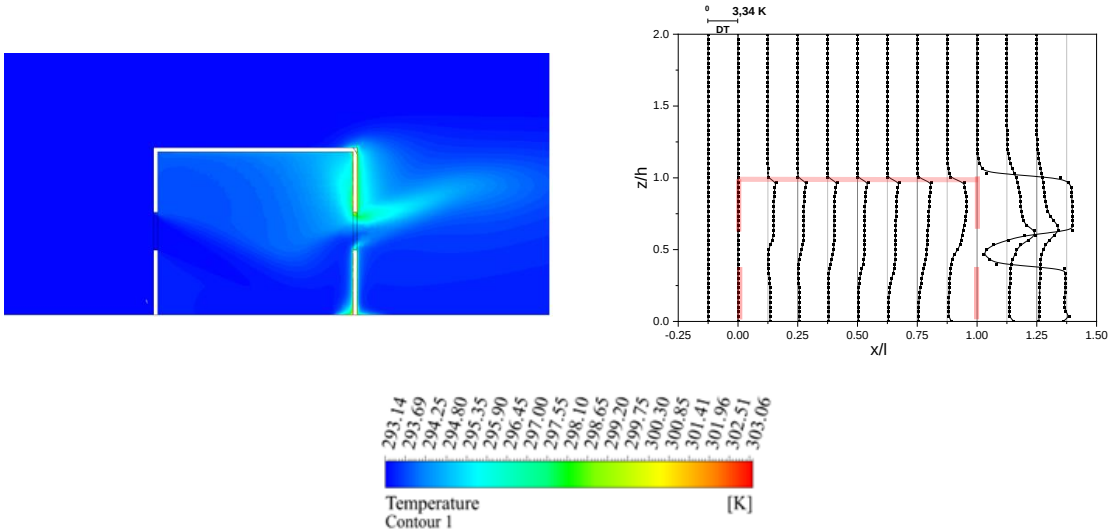

Fig. 9 – Cross sectional view of temperature field, and profiles of temperature difference (ΔT) for seven line positions along the building on the central plane. a) x/l=0.125, b) x/l=0.25, c) x/l=0.375, d) x/l=0.5, e) x/l=0.625, f) x/l=0.75, g) x/l=0.875.

Figure 9 shows a cross-sectional view of the temperature field and temperature difference (DT) profiles for seven line positions along the building on the central plane. a) x / l = 0.125, b) x / l = 0.25, c) x / l = 0.375, d) x / l = 0.5, e) x / l = 0.625, f) x / l = 0.75, g) x / l = 0.875. For the four configurations, including the isothermal reference case, the average wind flows are represented by the current lines in Figure 9. In both cases where the building ceiling outside and inside or the leeward wall outside and inside is heated (Figure. 9.1, 9.3) the flow shape is quite similar to the isothermal case, although the intensity of the vortex is slightly increased. When the wall facing the wind is warm, the buoyancy flow is moving up on the length of the wall and thus increases the vertical flow compared to the equal status. On the contrary, when the windward wall is warmer than the air, the upward buoyant flow opposes the downward oriented horizontal flow along this wall; Thus the flow structure is divided into two different areas and the area is well centered in the building (Fig. 9.2). Therefore, in the first three configurations, the flows exhibit the characteristic feature of a skimmed flow regime with one vortex while in the fourth case the flow resembles a skimmed flow regime with several vortices. It therefore appears that wall heating can generate significant changes in the flow regime.

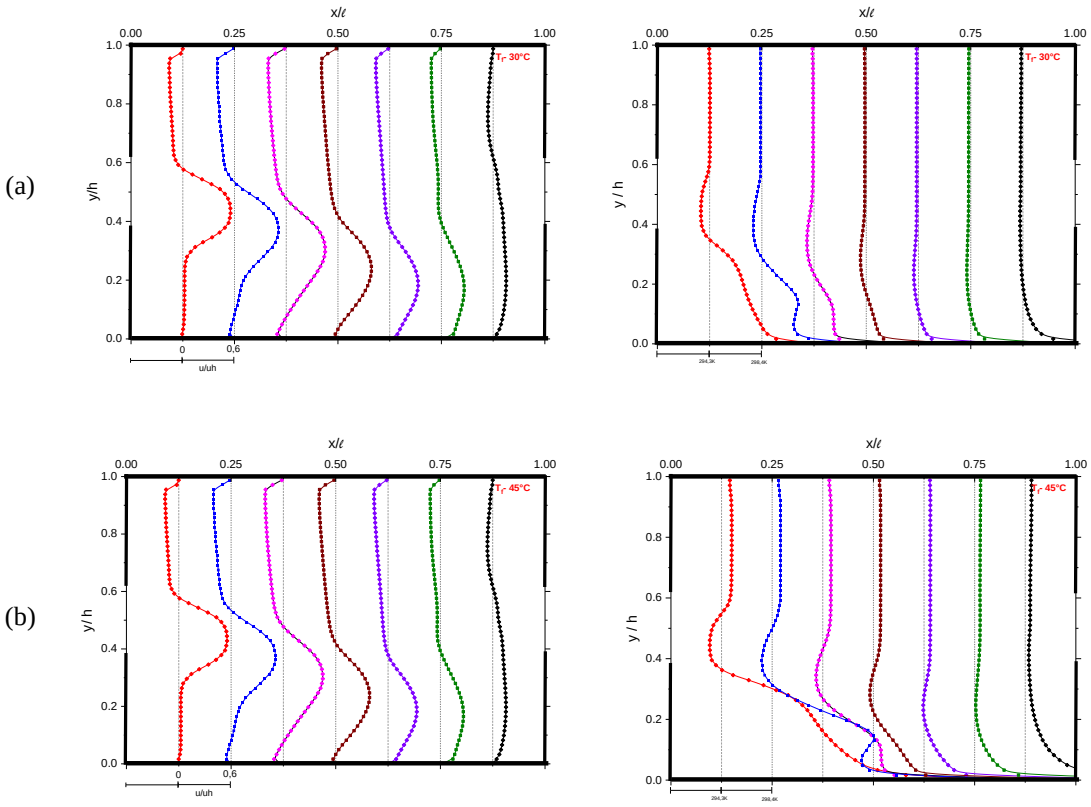

Fig. 10 – Comparison of vertical profiles of velocity (u/uh) and temperature (T) of numerical simulation; (a) Ta=20°C and Tf=30°C, (b) Ta=20°C and Tf=45°C, for seven line positions along the building on the central plane. a) x/l=0.125, b) x/l=0.25, c) x/l=0.375, d) x/l=0.5, e) x/l=0.625, f) x/l=0.75, g) x/l=0.875.

5 Presentation of the second part

The aim of this part of the thermal study is to determine the final results of cooling or heating a building from the inside in order to present serious solutions to this problem. For that, we made several numerical simulations concerning thermal part by software ANSYS CFX. the first case we have each time changed the air temperature and fixed the indoor floor temperature for an insulated building [(Ta = 55 ° C and Tf = 20 ° C), (Ta = 40 ° C and Tf = 20 ° C)], the second case we have fixed the two temperatures of the air and the indoor floor temperature (Ta = 20 ° C and Tf = 20 ° C) and the third case we have fixed the temperature of the air and changed each times the indoor floor temperature [(Ta = 20 ° C and Tf = 30 ° C), (Ta = 20 ° C and Tf = 45 ° C)], after that we plotted the curves for seven line positions along the building centrally. a) x / l = 0.125, b) x / l = 0.25, c) x / l = 0.375, d) x / l = 0.5, e) x / l = 0.625, f) x / l = 0.75, g) x / l = 0.875. An analysis of the speed change of the two thermal simulation cases is presented later.

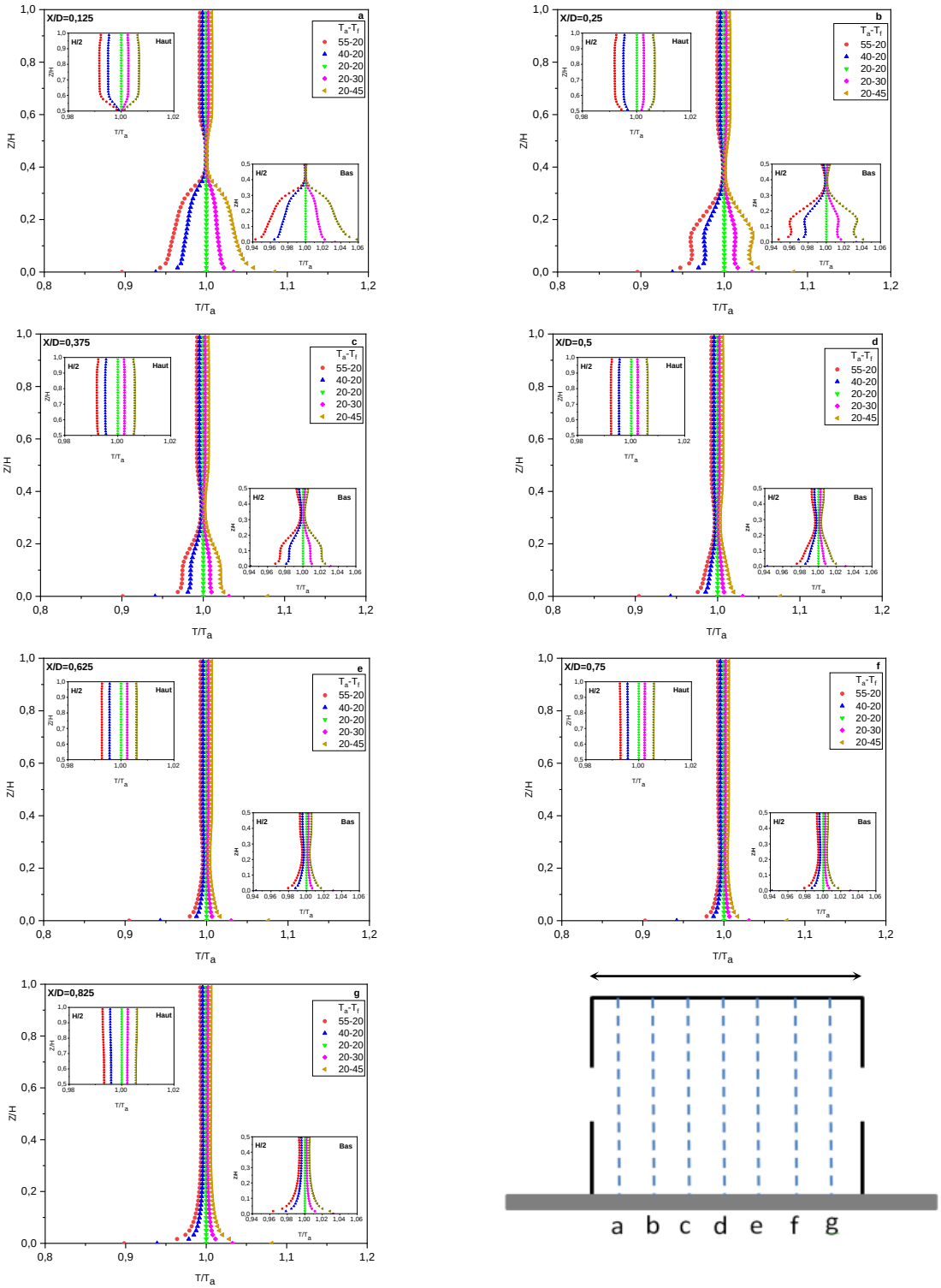

Fig. 11 – Comparison Different profiles of the rate temperature (T/Ta); (1) Ta=55°C and Tf=20°C, (2) Ta=40°C and Tf=20°C, (3) Ta=20°C and Tf=20°C, (4) Ta=20°C and Tf=30°Cand (5) Ta=20°C and Tf=45°C for seven line positions along the building on the central plane. a) x/l=0.125, b) x/l=0.25, c) x/l=0.375, d) x/l=0.5, e) x/l=0.625, f) x/l=0.75, g) x/l=0.875.

5.1 Results and discussion

Figure 10 is the results of plotting the temperature and dimensionless velocity profiles U/Uh for the two cases of the simulation of Tf = 30°C and Tf = 45°C. We noticed a change the temperature along seven line points only inside the building is shown in the figure. The difference between the results of the simulations (Tf =30 and 45°C) is clear, so that the horizontal temperature difference is less weak for Tf = 30 °C and it is important that Tf reaches 45°C. On the other hand, the region of minimum air temperature values for each floor temperature inside the building follows the direction of air flow. The change in speed along a building is almost the same as when Tf =20 °C. The vertical differences of temperature are more or less important at the intel region inside the building, the minimum value of this gradient is at maximum value of the velocity in flow direction, and the main temperature increase also in the flow direction. There is not a remarkable change in the profiles of the horizontal component of velocity when the floor temperature at Tf goes from 30 to 45 ° C. The figure shows that starting from z/h = 0.2the profiles have a almost right line form but beyond this z/h value there is a velocity difference, this is automatically due to the effect buoyancy on the cross ventilation flow. In general, the temperature of seven linear sites along the building at the central level, that each time we move away from the air inlet site we find that the temperature begins to decrease. shrink and approach for (Ta) until it reaches the location of the air outlet of the window and Starting from height z/h = 0.2 even the roof of the building, i.e. the temperature inside the building is near the air temperature (T ≈ Ta).

The figure 11 shows vertical profiles normalized to temperature ratios for seven line positions along the building on the central plane. a) x / l = 0.125, b) x / l = 0.25, c) x / l = 0.375, d) x / l = 0.5, e) x / l = 0.625, f) x / l = 0.75, g) x / l = 0.875.

This is why, at first, we increased air temperature (40 ° C to 55 ° C) and set the indoor floor temperature for an insulated building at (20 °C), that is to say heat the insulated building with air. As for the second step of this study, we fixed the air temperature at (20 °C) and we increased the indoor floor temperature for an insulated building from (30 ° C to 45 ° C), which means that the insulated building is cooled with air. At first, when the hot air collides with the facade of the building from the outside and enters through the window, we notice that the air has taken a downward current and formed a vortex of hot air and collided with the facade of the indoor floor for an insulated building, which means that the speed and direction of the air and the density also have a fundamental role in the heating of the building. In the figure, we notice each time that the air temperature is very large over the indoor floor temperature each time the temperature ratio is very small (T/Ta<1) and c ' is what is observed on the lower side of the curves and this is due to the role of the direction of the air inside the building downwards and the formation of an air vortex. Which directly leads to a gradual increase in temperature, unlike the upper face inside the building, and whenever the air temperature decreases and the indoor floor temperature decreases, the temperature ratio is approximately (T / Ta ≈ 1). In other words, the temperature and density of the air also play a vital role in heating the building.

In a second step, when the cold air collides with the facade of the building from and towards the outside and enters through the window, one notices that the air has taken a flow also downwards and formed a vortex the hot air and struck the indoor floor for an insulated building, that is, the speed, direction and density of the air also have a role. It is essential for cooling a building, so the faster the air, the slower the building cools, and vice versa. We notice whenever the air temperature is very small compared to the indoor floor temperature, the temperature ratio is very large (T / Ta >> 1) and it is this that we notice at the bottom of the curves this is due to the role of the direction of the air inside the building downwards and the formation of an air vortex, which directly leads to a gradual decrease in the temperature unlike the upper face inside the building, and whenever the air temperature increases and indoor floor temperature, the temperature ratio is close to (T / Ta ≈ 1), which means that the air temperature and its speed have a fundamental role in cooling the building.

Figure 11 also shows That the air temperature is equal to the indoor floor temperature (Ta = Tf), the temperature is almost 20 °C in the jet region, so the temperature of the air inside is almost equal to the air temperature outside, certainly his is due to the coming fresh outside air. finally, in general, that the temperature ratios of seven linear sites along the building at the central level, that each time we move away from the air inlet site we find that the temperature ratio begins to decrease. shrink and approach one (T / Ta ≈ 1) until it reaches the location of the air outlet of the window, i.e. the temperature inside the building is near the air temperature (T ≈ Ta).

6 Conclusion

In this paper the air quality inside and around isolated building is studied numerically using the kω-SST turbulence model implemented in the code ANSYS CFX, assuming a tree dimension, incompressible and stationary flow. The dynamics parameters of the flow (velocity and turbulent kinematic energy) are compared and validated with the available experimental data, it has shown a good agreement for the velocity and less good for kinematic turbulence energy, due to the excessive production of turbulent kinematic energy introduced by the turbulence model near the stagnation points.

During the day and due to the sun positions building walls temperature change, the numerical results show that the flow dynamic inside the building don't change with the walls temperature changing. counter to velocity the temperature distribution inside and outside is influenced by heated walls, when the roof is heated the upper air region of the building is heated and lock up due to upper vortex, in the second case, when the windward is heated a quantity of heated air stay under the coming jet from outside, in the last case of leeward walls heating the heated air is ejected outside the building by the output jet. The air temperature inside the building is match influenced by the floor temperature change, the vertical profiles of temperature show a decreasing of temperature gradients until the central zone when the inlet jet come white the fresh air of outside. After this zone, the deference slightly increases again and remains almost constant.

Notations

L	Length of rectangle (domain), m	u^*	Friction velocity, $\mathrm{m/s}$
W	Width of rectangle (domain), m	U_h	Wind tunnel speed , $\mathrm{m/s}$
H	Height of rectangle (domain), m	U	Average speed, $\mathrm{m/s}$
l	External length of cube, m	k	Turbulent kinetic energy,$\mathrm{m^2/s^2}$
w	External width of cube, m	ε	Energy dissipation at the inflow
h	External height of cube, m	T	Mean temperature, °C
h_0	Width of the opening (cube), m	ΔT	Temperature difference, °C
w_0	Height of the opening (cube), m	T_a	Ambient temperature of air, °C
e	Wall thickness, m	T_w	Temperature of wall, °C
z_0	Roughness parameter, mm	T_f	Floor temperature, °C
κ	Von Karman constant = 0.42	g	Acceleration due to gravity, $\mathrm{m/s^2}$

Acknowledgments

This work is supported by the Algerian General Direction of Scientific research and Technologic Development (DGRSDT).

REFERENCES

[1]- G.M. Stavrakakis, M.K. Koukou, M.G. Vrachopoulos, N.C. Markatos, Natural cross-ventilation in buildings: Building-scale experiments, numerical simulation and thermal comfort evaluation. Energ. Build. 40(9) (2008) 1666-1681. doi:10.1016/j.enbuild.2008.02.022.

[2]- K. Sato, T. Kurabuchi, T. Ogasawara, M. Ohba, S. Iwamoto, N. Sahashi, S. Ikehara, A Study on the Convective Heat Transfer Coefficient and Thermal Resistance of Clothing under Cross Ventilation. Int. J. Ventil. 10(2) (2011) 155-162. doi:10.1080/14733315.2011.11683944.

[3]- M.A. Del Rio, T. Asawa, Y. Hirayama, R. Sato, I. Ohta, Evaluation of passive cooling methods to improve microclimate for natural ventilation of a house during summer. Build. Environ. 149 (2019) 275-287. doi:10.1016/j.buildenv.2018.12.027.

[4]- S. Hawendi, S. Gao, A.Q. Ahmed, Effect of heat loads and furniture on the thermal comfort of an isolated family house under a naturally ventilated environment. Int. J. Ventil. 19(3) (2020) 163-188. doi:10.1080/14733315.2019.1600815.

[5]- Y. Zhao, L.W. Chew, A. Kubilay, J. Carmeliet, Isothermal and non-isothermal flow in street canyons: A review from theoretical, experimental and numerical perspectives. Build. Environ. 184 (2020) 107163. doi:10.1016/j.buildenv.2020.107163.

[6]- Y. Wang, T. Zhao, Z. Cao, C. Zhai, S. Wu, C. Zhang, Q. Zhang, W. Lv, The influence of indoor thermal conditions on ventilation flow and pollutant dispersion in downstream industrial workshop. Build. Environ. 187 (2021) 107400. doi:10.1016/j.buildenv.2020.107400.

[7]- Y. Vaishnani, S.F. Ali, A. Joshi, D. Rakshit, F. Wang, Thermal performance analysis of a naturally ventilated system using PMV models for different roof inclinations in composite climatic conditions. J. Bra. Soc. Mech. Sci. Eng. 42(3) (2020) 124. doi:10.1007/s40430-020-2219-4.

[8]- L. Chen, J. Hang, G. Chen, S. Liu, Y. Lin, M. Mattsson, M. Sandberg, H. Ling, Numerical investigations of wind and thermal environment in 2D scaled street canyons with various aspect ratios and solar wall heating. Build. Environ. 190 (2021) 107525. doi:10.1016/j.buildenv.2020.107525.

[9]- M.P. Straw, C.J. Baker, A.P. Robertson, Experimental measurements and computations of the wind-induced ventilation of a cubic structure. J. Wind Eng. Indust. Aerodyn. 88(2) (2000) 213-230. doi:10.1016/S0167-6105(00)00050-7.

[10]- P. Karava, T. Stathopoulos, A.K. Athienitis, Wind-induced natural ventilation analysis. Solar Energy 81(1) (2007) 20-30. doi:10.1016/j.solener.2006.06.013.

[11]- Y. Tominaga, B. Blocken, Wind tunnel experiments on cross-ventilation flow of a generic building with contaminant dispersion in unsheltered and sheltered conditions. Build. Environ. 92 (2015) 452-461. doi:10.1016/j.buildenv.2015.05.026.

[12]- Y. Tominaga, B. Blocken, Wind tunnel analysis of flow and dispersion in cross-ventilated isolated buildings: Impact of opening positions. J. Wind Eng. Indust. Aerodyn. 155 (2016) 74-88. doi:10.1016/j.jweia.2016.05.007.

[13]- N. Ikegaya, S. Hasegawa, A. Hagishima, Time-resolved particle image velocimetry for cross-ventilation flow of generic block sheltered by urban-like block arrays. Build. Environ. 147 (2019) 132-145. doi:10.1016/j.buildenv.2018.10.015.

[14]- M. Shirzadi, Y. Tominaga, P.A. Mirzaei, Wind tunnel experiments on cross-ventilation flow of a generic sheltered building in urban areas. Build. Environ. 158 (2019) 60-72. doi:10.1016/j.buildenv.2019.04.057.

[15]- T. van Hooff, B. Blocken, Y. Tominaga, On the accuracy of CFD simulations of cross-ventilation flows for a generic isolated building: Comparison of RANS, LES and experiments. Build. Environ. 114 (2017) 148-165. doi:10.1016/j.buildenv.2016.12.019.

[16]- J.I. Peren, T. van Hooff, R. Ramponi, B. Blocken, B.C.C. Leite, Impact of roof geometry of an isolated leeward sawtooth roof building on cross-ventilation: Straight, concave, hybrid or convex? J. Wind Eng. Indust. Aerodyn. 145 (2015) 102-114. doi:10.1016/j.jweia.2015.05.014.

[17]- J.I. Perén, T. van Hooff, B.C.C. Leite, B. Blocken, Impact of eaves on cross-ventilation of a generic isolated leeward sawtooth roof building: Windward eaves, leeward eaves and eaves inclination. Build. Environ. 92 (2015) 578-590. doi:10.1016/j.buildenv.2015.05.011.

[18]- K. Kosutova, T. van Hooff, C. Vanderwel, B. Blocken, J. Hensen, Cross-ventilation in a generic isolated building equipped with louvers: Wind-tunnel experiments and CFD simulations. Build. Environ. 154 (2019) 263-280. doi:10.1016/j.buildenv.2019.03.019.

[19]- C. Ooi, P.-H. Chiu, V. Raghavan, S. Wan, H.J. Poh, Porous media representation of louvers in building simulations for natural ventilation. J. Build. Perform. Simul. 12(4) (2019) 494-503. doi:10.1080/19401493.2018.1510544.

[20]- Y. Arinami, S.-i. Akabayashi, Y. Tominaga, J. Sakaguchi, Performance evaluation of single-sided natural ventilation for generic building using large-eddy simulations: Effect of guide vanes and adjacent obstacles. Build. Environ. 154 (2019) 68-80. doi:10.1016/j.buildenv.2019.01.021.

[21]- M. Bendida, A. Djellouli, D. Hamidat, M. Bouzit, Structure of the out-flows behind buildings and Influence of the geometry of the streets on the out-flows. J. Mater. Eng. Struct. 6(3) (2019) 375-382.

[22]- A.K. Hussein, A. Walunj, L. Kolsi, Applications of nanotechnology to enhance the performance of the direct absorption solar collectors. J. Thermal Eng. 2(1) (2016) 529-540.

[23]- A.K. Hussein, Applications of nanotechnology to improve the performance of solar collectors – Recent advances and overview. Renew. Sust. Energy Rev. 62 (2016) 767-792. doi:10.1016/j.rser.2016.04.050.

[24]- E. Khalid, O. Younis, A.M. Hamdan, A.K. Hussein, A Study on Energy Performance and Optimum Thickness of Thermal Insulation for Building in Different Climatic Regions in Sudan. J. Adv. Res. Fluid Mech. Thermal Sci. 73(2) (2021) 146-162.